The severe von Willebrand disease variant p.M771V leads to impaired anterograde trafficking of von Willebrand factor in patient-derived and base-edited endothelial colony-forming cells

Bär, I.; Barraclough, A.; Bürgisser, P.E.; Kwawegen, C. van; Fijnvandraat, K.; Eikenboom, J.C.J.; ... ; Bierings, R.

Citation

Note: To cite this publication please use the final published version (if applicable).

jth

ORIGINAL ARTICLE

The severe von Willebrand disease variant p.M771V leads to impaired anterograde trafficking of von Willebrand factor in patient-derived and base-edited endothelial colony-forming cells

Isabel Bär[1] ✕ | Alastair Barraclough[2] | Petra E. Bürgisser[1] |
Calvin van Kwawegen[1] | Karin Fijnvandraat[2] | Jeroen C. J. Eikenboom[3] |
Frank W. G. Leebeek[1] ✕ | Jan Voorberg[4] ✕ | Ruben Bierings[1] 🔟 ✕ ✕ ✕

[1]Department of Hematology, Erasmus University Medical Centre, Rotterdam, The Netherlands

[2]Department of Pediatric Hematology, Emma Children's Hospital, Amsterdam UMC, University of Amsterdam, Amsterdam, The Netherlands

[3]Department of Internal Medicine, Division of Thrombosis and Hemostasis, Leiden University Medical Centre, Leiden, The Netherlands

[4]Molecular Hematology, Sanquin Research and Landsteiner Laboratory, Amsterdam University Medical Centre, Amsterdam, The Netherlands

Correspondence
Ruben Bierings, Department of Hematology, Erasmus University Medical Centre, Rotterdam, The Netherlands.
Email: r.bierings@erasmusmc.nl

Abstract

Background: von Willebrand disease (VWD) is the most common inherited bleeding disorder caused by quantitative or qualitative defects in von Willebrand factor (VWF). The p.M771V VWF variant leads to a severe bleeding phenotype in homozygous patients. However, the exact molecular mechanism remains unclear, which prevents personalized treatment of those VWD patients.

Objectives: This study aimed to characterize the underlying molecular mechanisms of the p.M771V variant in multiple representative *ex vivo* cell models.

Methods: Endothelial colony-forming cells (ECFCs) were isolated from venous blood of VWD patients from the Willebrand in the Netherlands cohort carrying homozygous and heterozygous p.M771V VWF variants. The p.M771V variant was also introduced in cord blood-derived ECFCs (CB-ECFCs) through adenine base editing and was overexpressed in HEK293 cells. Biosynthesis, storage, and secretion of VWF was studied using biochemical methods and confocal microscopy.

Results: Two unrelated homozygous p.M771V patients presented with very low VWF activity and antigen levels in plasma. Patient ECFCs showed impaired uncleaved VWF processing into mature VWF, with secreted VWF being severely reduced when compared to ECFCs of healthy donors. Multimer analysis of p.M771V ECFCs showed a deficiency of high molecular weight VWF multimers. Immunofluorescent staining revealed VWF retention in the endoplasmic reticulum; this was confirmed in various populations of base-edited CB-ECFCs harboring the p.M771V variant.

Conclusion: The severe endothelial phenotype observed in patient-derived p.M771V ECFCs, HEK293 cells, and an original base-edited CB-ECFC modeling system show that

endoplasmic reticulum retention of VWF and failure to undergo subsequent proteolytic processing underpins the severe bleeding phenotype of patients with homozygous variants at M771.

1 | INTRODUCTION

von Willebrand factor (VWF) is a multimeric protein circulating in the bloodstream that plays a fundamental role in primary hemostasis. The primary role of VWF is to tether platelets by catch bond-dependent interactions with glycoprotein Ib on platelets from circulating blood at sites of vascular injury [1]. In addition, VWF serves as a chaperone for factor VIII (FVIII), protecting it from premature clearance, thereby preventing bleeding [2]. VWF is synthesized and stored in specific organelles, namely Weibel-Palade bodies (WPBs) in endothelial cells and α-granules in megakaryocytes [3]. Upon its entry into the endoplasmic reticulum (ER), the signal peptide is removed from the pre-proVWF; within the lumen of the ER, proVWF undergoes N-linked glycosylation as well as dimerization via its cysteine knot domain [4]. Following its transfer to the Golgi apparatus, the acidic environment and high Ca^{2+} concentration promotes the formation of large multimers that are formed through N-terminal interchain disulfide bonds that have been proposed to be catalyzed by the VWF propeptide (VWFpp). In the trans-Golgi apparatus, proVWF is cleaved at the R763-S764 peptide bond adjacent to the D' domain, thereby separating VWFpp and mature VWF. The resulting mature VWF multimers are then packed and stored in WPBs and are released via the basal secretion pathway or upon stimulation [5]. A small fraction of low molecular weight (LMW) VWF enters the secretory pathway directly and is constitutively secreted. However, high molecular weight (HMW) VWF is far more efficient in recruiting platelets, and WPB-stored VWF multimers are therefore considered to be crucial for hemostasis.

Mutations in the VWF gene (*VWF*) lead to quantitative, structural, or functional abnormalities that present in patients as different types of von Willebrand disease (VWD) [6]. VWD is the most common inherited bleeding disorder in humans with a prevalence of up to 1% in the general population. Depending on the underlying variant, VWD presents with a variety of symptoms including mucosal bleeds, menorrhagia, and bleeding after surgery or trauma, which affects the patients' quality of life [7]. The Willebrand in the Netherlands (WiN) study revealed multiple missense variants in *VWF* of VWD patients in the Netherlands [8]. Two unrelated patients with a homozygous p.M771V variant presented with a very severe bleeding phenotype, including low to nondetectable VWF levels in plasma and frequent hospital visits. The p.M771V variant is located in the D' domain of *VWF*, which is close to the furin cleavage site at R763 and within the

FVIII binding region in the D3 domain [9]. Here, we explore the molecular mechanism resulting from the p.M771V variant in patient-derived endothelial colony-forming cells (ECFCs). The findings obtained show that the p.M771V variant induces defective processing of proVWF and lack of stored HMW VWF multimers, providing insights into the underlying mechanism of the VWD phenotype.

Although the clinical manifestation of VWD differs greatly between patients depending, among other factors, on their VWF variant, treatment is currently mostly provided as either factor concentrates or DDAVP/desmopressin administration [7,10]. While these therapies benefit the majority of patients, they only provide short-term solutions on demand. In case of a severe bleeding phenotype, as in VWD type 3 patients, patients need to constantly be aware of their disease and require regular hospital visits to receive (prophylactic) treatment. A more personalized treatment on a genetic or specific molecular level would ease the disease burden for these patients. However, the large number and heterogeneity of genetic variants associated with VWD complicates the understanding of the underlying pathomolecular mechanism and the diagnosis of VWD [8]. Providing deeper insights into the consequences of missense variants in various parts of *VWF* is a first step toward the development of better therapeutic strategies for VWD patients. In this study we show various ways to characterize a *VWF* variant, in our case p.M771V. We first deployed a HEK293 overexpression model expressing p.M771V or wild type (WT) VWF to bypass patient epigenetic factors. In a parallel approach, we developed a Cas9-based adenine base editor to introduce the p.M771V substitution in cord blood ECFCs (CB-ECFCs) to observe the phenotype caused by the variant in an endothelial cell system. Thereby, we demonstrated an advanced technique for modeling VWD in ECFCs, potentially acting as a relevant surrogate model when patient-derived material is not available. Unraveling the molecular mechanisms caused by VWF variants will help diagnose patients and drive the development of new therapeutic approaches tailored to the needs and phenotype of people with VWD.

2 | METHODS

2.1 | Patient cohort and sequencing data

All patients were selected from the WiN-Pro study (Willebrand in the Netherlands study). The WiN-Pro study is an ongoing nationwide,

multicenter, prospective cohort study in patients with VWD (ClinicalTrials.gov: NCT03521583), which started recruitment in July 2019. More information on the inclusion criteria and laboratory measurements for the patients can be found in the Supplementary Material (WiN-Pro study).

All patients and healthy controls gave informed consent to study their ECFCs, CB-ECFCs, and human umbilical vein endothelial cells (HUVECs) in the BOEC-MK-2020 study in accordance with the Declaration of Helsinki. Next generation sequencing (NGS) of the complete *VWF* including exonic and intronic regions was performed in the WiN-Pro study by Illumina NovaSeq.

2.2 | Cell culture and isolation of endothelial cells

ECFCs were isolated from the peripheral blood of patients as previously described [11]. CB-ECFCs were obtained from cord blood collected from umbilical veins within 24 hours after delivery [12]. Isolation of HUVECs from the same umbilical cords was accomplished by subsequent flushing of the umbilical veins with 0.05% trypsin-EDTA as described previously [13]. HUVECs, CB-ECFCs, and ECFCs were cultured on 1% gelatin-coated dishes in EGM-2 (Promocell, C22111) supplemented with 18% fetal calf serum (FCS; Bodinco), 5% penicillin/streptomycin, and the endothelial growth medium supplements provided by Promocell. Cells were cultured at 37 °C in a humified atmosphere of 5% CO_2 and passaged every 2 to 3 days at a confluency of 80% to 90% to maintain proliferation using 0.05% trypsin-EDTA. ECFCs were used for experiments before passage 10 to avoid influences by changes of VWF production of older cells. HEK293 (DSMZ, Leibniz Institute) and HEK293T (ATCC) cells were cultured in Dulbecco's modified Eagle medium containing D-glucose and L-glutamine (Thermo Fisher Scientific, 11965092), supplemented with 10% FCS and 5% penicillin/streptomycin. For single cell sorting of base-edited ECFCs, cells were detached with 0.05% trypsin-EDTA and resuspended in Ca- and Mg-free phosphate-buffered saline (PBS) with 1% FCS and stained with LIVE/DEAD marker (Thermo Fisher Scientific, L34975). Single cell sorting was performed on a BD FACSAria Cell Sorter using a 100 μm nozzle at a pressure of 20 PSI. After sorting, cells were maintained in growth conditions for 1 week. Media was refreshed 3 times per week with passaging occurring at 80% to 100% confluency.

2.3 | Immunocytochemistry staining and confocal analysis

Cells were fixed with 4% paraformaldehyde in PBS for 15 minutes at room temperature before washing and blocking in Perm/Quench (50 mM NH_4Cl, 0.2% w/v saponin in PBS). After 10 to 15 minutes, the samples were washed and stored in PGAS (0.2% w/v gelatin, 0.02% w/v saponin, 0.02% w/v NaN_3 in PBS) until staining. Staining was performed in PGAS with the antibodies mentioned in Supplementary Tables 1 and 2. Imaging was performed on the Zeiss LSM 980 Airyscan with a Plan-Apochromat 63×/1.40 oil DIC M27 objective (Zeiss, 420782-9900-000) or on the Leica SP8 and Zeiss Elyra PS.1 SIM, capturing around 20 Z-slices per image. The images were analyzed using Zen Blue (version 3.3) or ImageJ-based processing workflows, respectively. Pearson's colocalization coefficient was determined for VWF and protein disulfide isomerase (PDI) using the JACoP plugin in ImageJ [14,15]. Tile scans were acquired using Leica Stellaris 5 LIA. Quantitative analysis of WPB morphometry from tile scans of CB-ECFCs and HUVECs was performed using the CellProfiler software pipeline published by Laan et al. [16].

2.4 | ELISA

Supernatant samples of ECFCs were tested for secreted VWF using ELISA assay. Plates were coated with DAKO AB (Supplementary Figure 1) overnight. Samples were measured in duplicate and with various dilutions.

2.5 | Multimer assay and densitometry graphs

Supernatants and lysates of cells were used for visualization of VWF multimer patterns. Samples in Tris/EDTA and glycerol were heated to 60 °C for 20 minutes before electrophoresis on a 0.9% agarose gel at 75 V for 6 hours at 4 °C. The gel was then reduced in β-mercaptoethanol in PBS for 10 minutes on a shaker and subsequently washed with PBS. The gel was transferred to a 0.2 μm nitrocellulose membrane by capillary suction overnight. Multimer patterns were visualized using horseradish peroxidase-conjugated anti-VWF antibody and enhanced chemiluminescence assay solution using an Amersham Imager 600. ImageJ64 was used to translate the multimer pattern into densitometry graphics.

2.6 | Western blotting

Proteolytic processing of VWF and VWFpp was assessed essentially as described previously [17]. ECFCs were lysed in NP-40 buffer (5 mM EDTA pH 8.0, 10 mM Tris-HCl pH 6.7, 150 mM NaCl, 0.5% Igepal) supplemented with protease inhibitor (Sigma, S8820). Protein concentrations of lysate samples were quantified using the Pierce 660 nm protein assay. Equal protein concentrations of lysate samples were separated on a gradient Bis-Tris NuPAGE gels (Invitrogen, 4% to 12%) under reducing conditions and transferred to a 0.2 μm nitrocellulose membrane using wet-blotting. Protein detection was facilitated using rabbit polyclonal anti-VWF and rabbit polyclonal anti-VWFpp antibodies [18]. Dilutions are detailed in Supplementary Table 1. Membranes were visualized on an Odyssey Clx scanner (Li-COR).

2.7 | Cloning and nucleofection of VWF-WT and VWF-M771V

For overexpression of VWF WT and VWF p.M771V in HEK293 cells, the pcDNA3.1-VWF-WT plasmid was used and modified to introduce the p.M771V variant [19]. First, a 686 bp fragment containing the cytomegalovirus (CMV) enhancer and promoter cassette were removed by digestion with SpeI. Subsequently, the VWF sequence between restriction sites HindIII and BamHI was replaced by a 482 bp synthetic *VWF* DNA fragment containing the p.M771V variant (synthesized by Base-gene, Supplementary Table 3). The CMV enhancer and CMV promoter were reintroduced by insertion of a 1153 bp MfeI-BsrGI fragment from pcDNA3.1-VWF-WT into pcDNA3.1-VWF-M771V. The final construct was verified by Sanger sequencing.

Nucleofection of HEK293 cells was performed in a Lonza 4D Nucleofector using the Amaxa P5 primary Cell 4D Nucleofector x Kit (Lonza V4XP-5024). Two micrograms of plasmid DNA (pcDNA3.1-VWF-WT or pcDNA3.1-VWF-M771V) was used per condition to transfect 6×10^5 HEK293 cells. Cells were fixed and stained 3 days after nucleofection according to the protocol described above.

2.8 | Lentiviral transduction of base editors

For generation of lentiviral adenine base editing (ABE) vector (LV-SpG-ABE8e), the SpGCas9-ABE8e cassette was amplified from pCMV-T7-ABE8e-nSpG-P2A-EGFP, which was a gift from Benjamin Kleinstiver (Addgene plasmid #185911) [20]. The Cas9 cassette of Lenti-CRISPR-V2, which was a gift from Feng Zang (Addgene plasmid #52961) [21], was replaced with the aforementioned PCR product between restriction sites XbaI and BamHI. All sequences can be found in Supplementary Table 3. The guide RNA (gRNA) targeting the p.M771 locus was primarily selected based on the availability of a PAM sequence at a set distance away to ensure c.A2311 would fall into the predicted editing window of the base editor [20,22]. Secondary selection was based on low off-targeting scores obtained using CRISPOR [23]. Complementary oligos were obtained from Integrated DNA Technologies encoding the gRNA sequence with overhangs compatible with BsmBI sites between the U6 promoter and scaffold sequences on the LV-SpG-ABE8e vector. The oligos were annealed in a thermocycler at 95 °C for 5 minutes and cooled to room temperature before insertion in the BsmB1 site. The nucleotide sequence of the constructs used in this study is provided in the Supplementary Material.

For lentiviral production, HEK293T cells were triple transfected with psPAX2 (Addgene #12260), pMD2.G (Addgene #12259) and either LV-SpG-ABE8e-M771V or LV-SpG-ABE8e as a negative control. Viral harvests were performed 48 and 72 hours after polyethylenimine (Polysciences, 23966-100) transfection, pooled, and then concentrated via centrifugation at 35,000g for 2 hours at 4 °C (Sigma 3-30KS, 12158-H rotor). CB-ECFCs were transduced at passage 6 with either LV-SpG-ABE8-M771V or LV-SpG-ABE. Enrichment was achieved using puromycin selection at 1 μg/mL for 72 hours.

2.9 | Sequencing

Genomic DNA was extracted using the DNeasy Blood&Tissue kit (Qiagen, 69504) and quantified using a NanoDrop 2000/2000c Spectrophotometer (Thermo Scientific). PCR of the p.M771 loci was performed with Q5 polymerase (NEB, M0492L). PCR products were purified with Monarch PCR&DNA cleanup kits (NEB, T1030) followed by Sanger sequencing using the BigDye Terminator v3.1 Cycle Sequencing Kit (ThermoScientific). Snapgene (version 7.0.3) was used for alignment of the traces to the p.M771 loci. Quantification of Sanger sequencing was performed by EditR analysis [24]. For NGS sequencing, genomic DNA was amplified using primers with adapter extensions (Supplementary Table 3). Samples were sequenced on an Illumina MiSeq, and NGS analysis and quantification were performed using CRISPResso2 [25].

3 | RESULTS

3.1 | Phenotypic characterization of primary endothelial cells from VWD patients carrying the p.M771V variant

Homozygous and compound heterozygous missense variants in *VWF* have been associated with severe cases of VWD, but the pathogenic mechanisms that result in absence of VWF in plasma often remain unclear. A recent genotypic characterization of patients enrolled in the WiN study identified a large number of new *VWF* variants [8]. In that study, we identified 2 families (Figure 1A) with a severe bleeding phenotype carrying a homozygous c.2311A>G variant in exon 18, resulting in a p.M771V conversion in the VWF D' domain, 8 residues downstream of the proteolytic VWFpp furin cleavage site [26]. The affected homozygous p.M771V individuals show a high International Society on Thrombosis and Haemostasis ISTH Bleeding Assessment Tool score (Figure 1C) and low plasma values of VWF antigen (VWF:Ag), VWF activity (VWF:Act, VWF:GPIbM), and FVIII clotting activity (FVIII:C) (Figure 1B), which underpin the severity of the bleeding phenotype. While Persons 1 and 3 receive on-demand treatment, Persons 2 and 4 suffer from joint bleeds, which is why both have received prophylactic treatment in the past. While the treatment was reduced for patient 2 after a few years and switched to on-demand treatment, the dosage for patient 4 was even increased after her menarche. The parents of family 1 are not known in any Hemophilia treatment center and therefore considered to not have a bleeding phenotype. Person 7 was previously on prophylaxis but is now managing his bleeding with on-demand treatment. To investigate the pathogenic mechanism through which the p.M771V variant causes the severe bleeding phenotype, we isolated ECFCs from the venous blood of 3 individuals carrying this variant. In family 1, a p.R2663P variant cosegregated with the p.M771V variant but is not suspected to be the pathogenic driver of the resulting bleeding tendency. Both variants have been reported in the NCBI dbSNP database, but their functional effect has not yet been established. Venous blood ECFCs
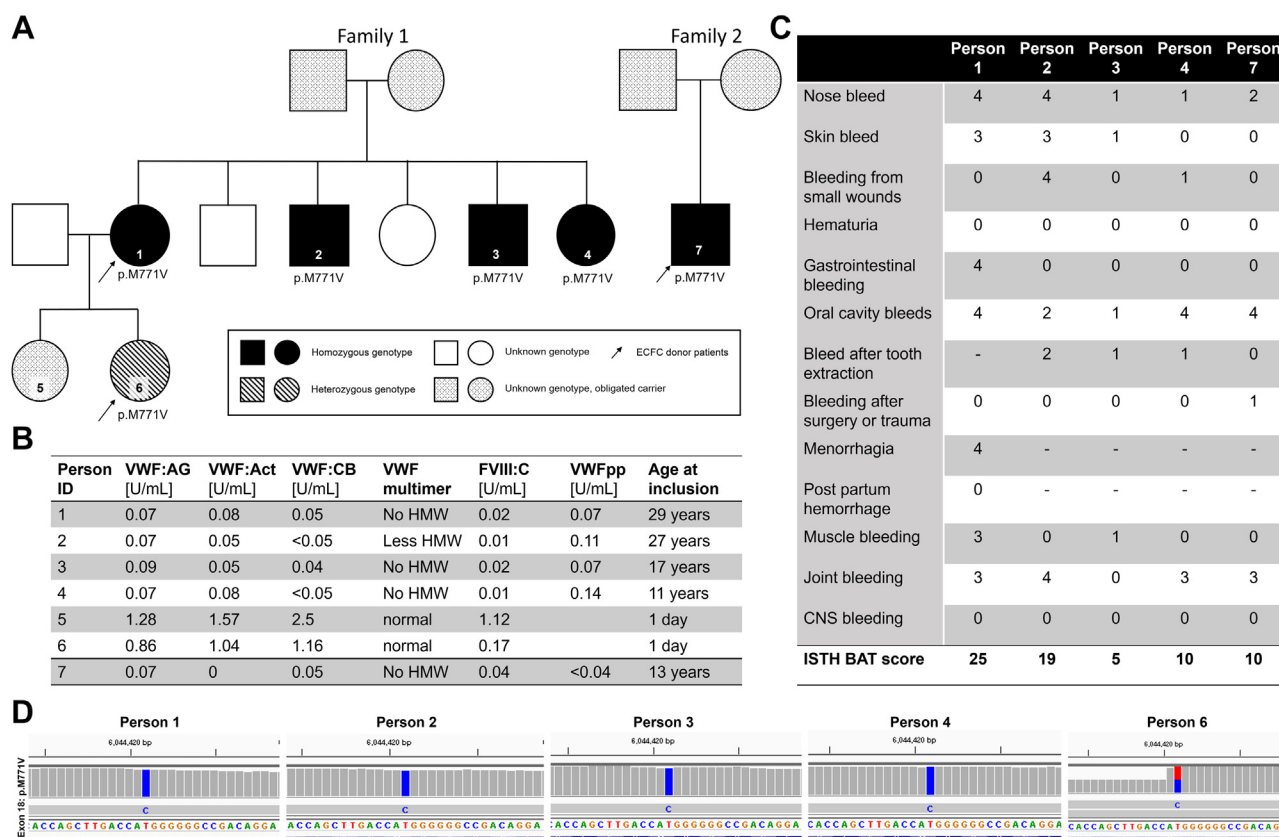
A Family 1 / Family 2

Homozygous genotype | Unknown genotype | ECFC donor patients
Heterozygous genotype | Unknown genotype, obligated carrier

B

Person ID	VWF:AG [U/mL]	VWF:Act [U/mL]	VWF:CB [U/mL]	VWF multimer	FVIII:C [U/mL]	VWFpp [U/mL]	Age at inclusion
1	0.07	0.08	0.05	No HMW	0.02	0.07	29 years
2	0.07	0.05	<0.05	Less HMW	0.01	0.11	27 years
3	0.09	0.05	0.04	No HMW	0.02	0.07	17 years
4	0.07	0.08	<0.05	No HMW	0.01	0.14	11 years
5	1.28	1.57	2.5	normal	1.12		1 day
6	0.86	1.04	1.16	normal	0.17		1 day
7	0.07	0	0.05	No HMW	0.04	<0.04	13 years

C

	Person 1	Person 2	Person 3	Person 4	Person 7
Nose bleed	4	4	1	1	2
Skin bleed	3	3	1	0	0
Bleeding from small wounds	0	4	0	1	0
Hematuria	0	0	0	0	0
Gastrointestinal bleeding	4	0	0	0	0
Oral cavity bleeds	4	2	1	4	4
Bleed after tooth extraction	-	2	1	1	0
Bleeding after surgery or trauma	0	0	0	0	1
Menorrhagia	4	-	-	-	-
Post partum hemorrhage	0	-	-	-	-
Muscle bleeding	3	0	1	0	0
Joint bleeding	3	4	0	3	3
CNS bleeding	0	0	0	0	0
ISTH BAT score	25	19	5	10	10

D Person 1 / Person 2 / Person 3 / Person 4 / Person 6

FIGURE 1 Clinical presentation of 2 families carrying the p.M771V variant. (A) Family relations of patients carrying a p.M771V variant. (B) Venous blood plasma measurements of clinical values at patient inclusion in the WiN study. (C) ISTH BAT bleeding score acquired upon patient inclusion in the WiN study (D) Next generation sequencing of *VWF* confirming p.M771V variant profile. CNS, central nervous system; ECFC, endothelial colony-forming cell; FVIII:C, factor VIII clotting activity; HMW, high molecular weight; ISTH BAT, International Society on Thrombosis and Haemostasis Bleeding Assessment Tool; VWF, von Willebrand factor; VWF:Act, VWF activity; VWF:AG, VWF antigen; VWF:CB, VWF collagen binding activity; VWFpp, VWF propeptide.

were isolated from Persons 1 and 7. HUVECs and CB-ECFCs had been isolated from the umbilical cord and cord blood from Person 6, the heterozygous offspring of Person 1. NGS confirmed the genotype of all study participants (Figure 1D).

Morphologic analysis using confocal microscopy revealed a severe VWF trafficking phenotype in the homozygous p.M771V ECFCs derived from Person 1, showing the absence of WPBs and retention of VWF within the ER as judged by colocalization of VWF with the ER marker PDI and shown by the Pearson's colocalization coefficient (Figure 2A). ER retention was also observed in the heterozygous p.M771V CB-ECFCs, even though some WPBs were present in this condition. Essentially similar observations were made in heterozygous p.M771V HUVECs (Figure 2B) [27]. The phenotypical characteristics of the heterozygous p.M771V ECFCs are concordant with higher VWF plasma levels of those individuals compared with the homozygous p.M771V patients. Due to their young age, lack of bleeding history, and intermediate plasma values, the heterozygous Person 1 has not been diagnosed with any type of VWD. However, the low FVIII values in the offspring, namely Person 6, suggest a VWD type 2N phenotype. To diagnose this person, a VWF:FVIII binding test (VWF:FVIIIB) needs to be

performed and the amount of bleeding needs to be assessed in this individual.

Previous reports have shown that a reduction of VWF synthesis or VWF trafficking through the early secretory pathway results in morphologic changes of WPBs, primarily loss of elongated shape and reduction in organelle length [28–31]. To quantitatively assess morphologic differences of WPBs produced in heterozygous ECFCs and WT ECFCs, we used our recently developed Cell Profiler pipeline to morphometrically analyze WPBs of >600 endothelial cells per tile scan (Figure 2C) [16]. This analysis revealed significant differences in general cell size (area) but especially regarding the length (max Ferret) and eccentricity of WPBs, which were significantly shorter and rounder in heterozygous p.M771V ECFCs compared to control donor ECFCs.

3.2 | Defects in proteolytic processing and multimerization of VWF p.M771V

To investigate potential changes in biosynthesis and posttranslational modification of VWF as a result of the p.M771V variant, lysates of homozygous and heterozygous ECFCs were analyzed for their
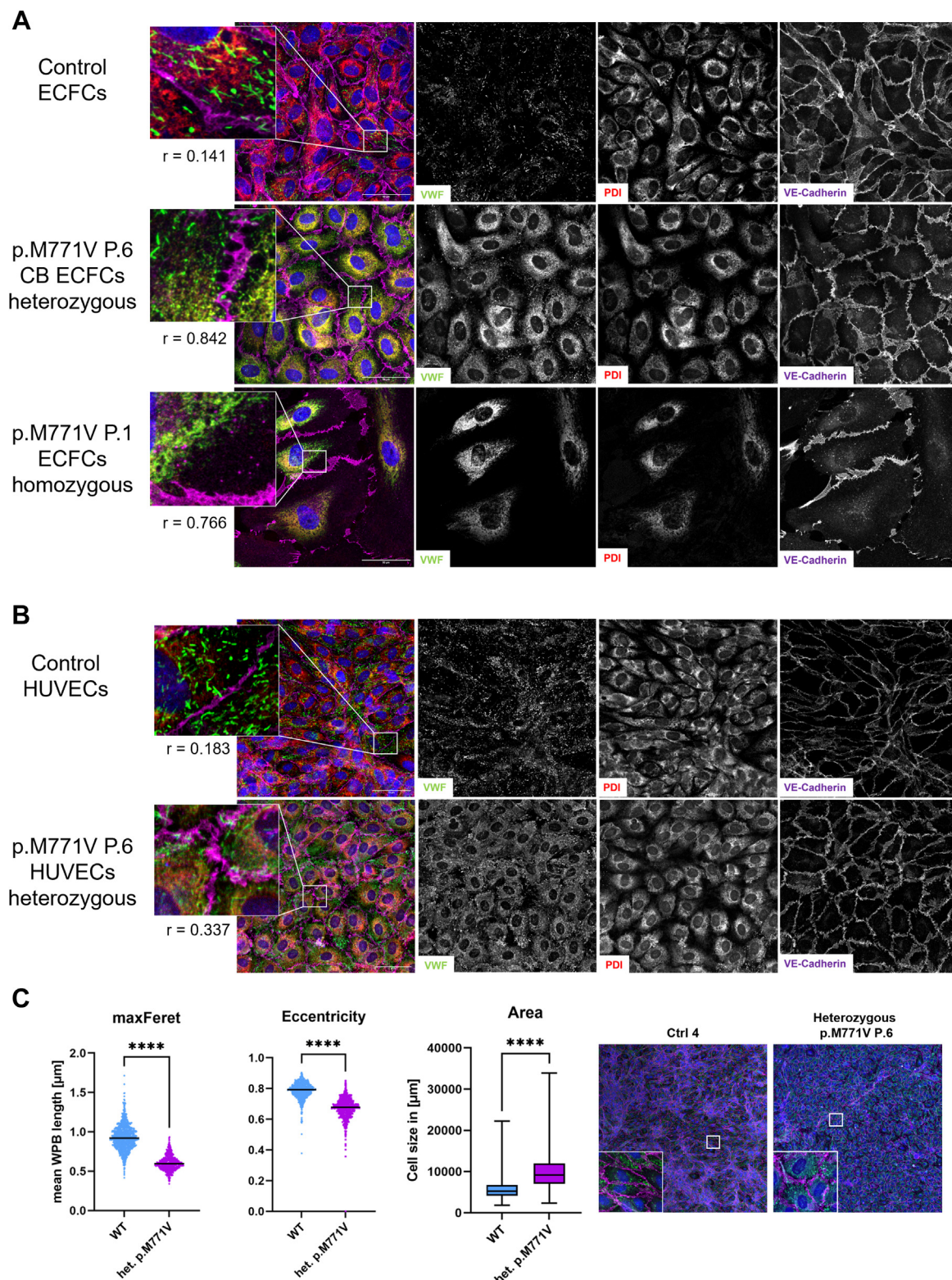
FIGURE 2 Phenotypic characterization of patient-derived endothelial cells. (A) ECFCs derived from venous blood of the patient show severe ER retention of VWF in a homozygous genotype. ECFCs derived from the umbilical CB of the heterozygous child of the patient show an intermediate phenotype. Colocalization analysis based on Pearson's correlation coefficient for VWF-PDI is indicated in the panels. B) Heterozygous HUVECs derived from the umbilical cord of the patient's child show the same phenotype as the corresponding CB-derived ECFCs. Magenta: VE-cadherin; Red: PDI; Green: VWF; scale bar 50 μm. (C) Analysis of WPBs of heterozygous p.M771V and WT CB-ECFCs using tile scans (shown on the right) of the respective conditions. WPBs are significantly shorter and rounder in heterozygous p.M771V CB-ECFCs, and the cells show a significant increase in size. Statistical analysis using Mann–Whitney U-test. ****$P < .0001$. CB, cord blood; ECFC, endothelial colony-forming cell; ER, endoplasmic reticulum; HUVEC, human umbilical vein endothelial cell; P, patient; PDI, protein disulfide isomerase; VE, vascular endothelial; VWF, von Willebrand factor; WPB, Weibel-Palade body; WT, wild type.
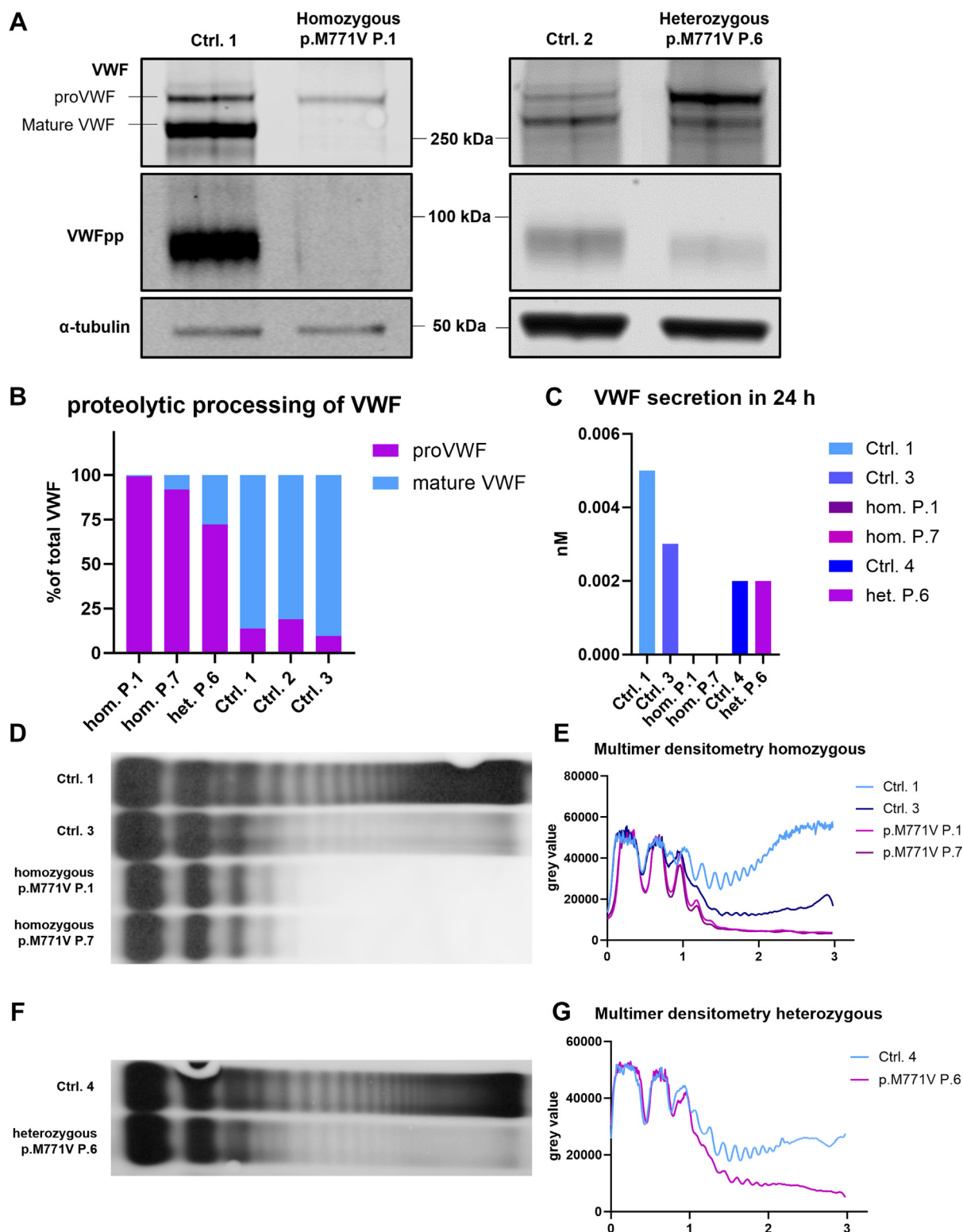
FIGURE 3 Molecular consequences of p.M771V variant. (A) Western blot of lysates from homozygous and heterozygous patient-derived ECFCs shows lack of mature VWF and VWFpp in homozygous and reduced amount of mature VWF and VWFpp in the heterozygous genotype. (B) p.M771V carriers show a high ratio of uncleaved (pro)VWF to mature VWF with almost complete lack of mature VWF in the homozygous ECFC lysates. (C) No secretion of VWF into culture medium could be detected within 24 hours in homoyzgous p.M771V ECFCs. The quantity of VWF secretion does not differ between heterozygous p.M771V ECFCs and WT ECFCs. (D) Multimer analysis of secreted VWF within 24 hours shows lack of HMW multimers in both homozygous patient-derived ECFCs. (E) Densitometry analysis confirms lack of HMW multimers in p.M771V ECFCs. (F) Multimer analysis of secreted VWF within 24 hours shows reduced HMW multimers in heterozygous CB-ECFCs compared to healthy CB-ECFCs. (G) Densitometry analysis confirms reduced amount of HMW multimers in heterozygous p.M771V CB-ECFCs. CB, cord blood; Ctrl, control; ECFC, endothelial colony-forming cell; het, heterozygous; hom, homozygous; HMW, high molecular weight; P, patient; PDI, protein disulfide isomerase; proVWF, uncleaved VWF; VWF, von Willebrand factor; VWFpp, von Willebrand factor propeptide; WPB, Weibel-Palade body; WT, wild type.
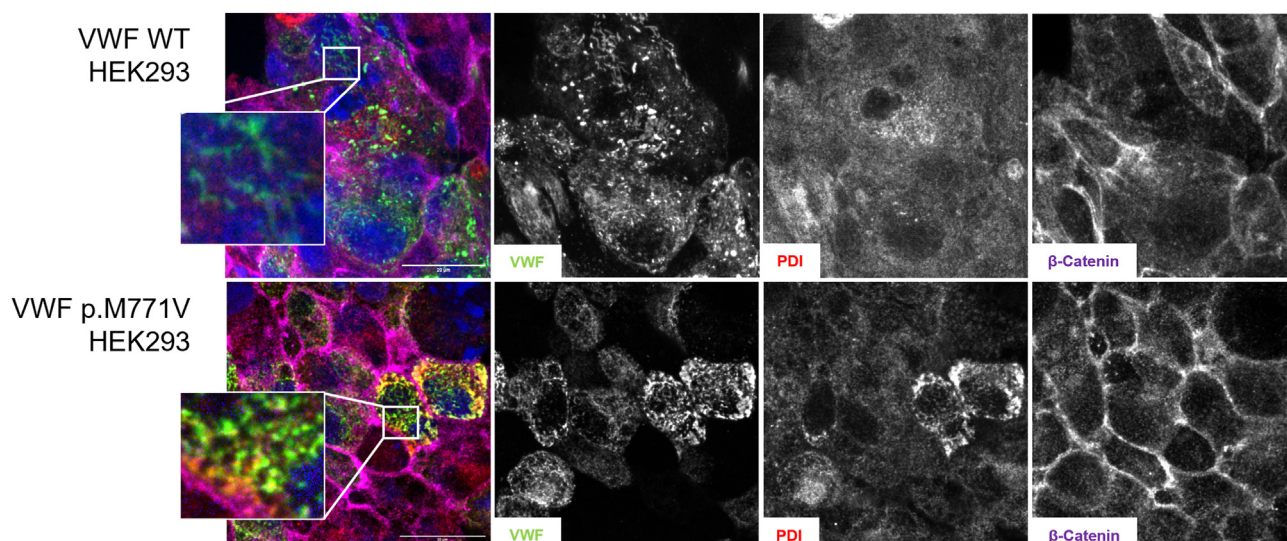
FIGURE 4 Ectopic expression of VWF and p.M771V VWF in HEK293 cells. (A) Ectopic expression of WT VWF leads to a pseudo-WPB expression in HEK293. Expression of VWF containing the p.M771V variant results in an unorganized structure of VWF colocalizing with the PDI staining. Magenta: β-catenin; Red: PDI; Green: VWF; scale bar 20 μm. PDI, protein disulfide isomerase; VWF, von Willebrand factor; WT, wild type.

proVWF, mature VWF, and VWFpp content (Figure 3A). Healthy control ECFCs were selected based on their growth speed and morphology *in vitro* to match the ECFC properties of the patient's cells. Molecular analysis of intracellular VWF suggested a proteolytic processing defect as a result of the p.M771V variant, evidenced by a shift from processed, mature VWF to unprocessed proVWF (Figure 3A). Quantitative analysis of VWF processing (Figure 3B) indicated that the majority of produced VWF seemed unable to convert into the mature form, which was also highlighted by the absence and strong reduction of intracellular VWFpp in the homozygous and heterozygous p.M771V ECFCs, respectively. Only ∼5% of VWF was further processed into mature VWF in the homozygous genotypes, while the mature VWF accounted for ∼85% of the total VWF content in healthy ECFCs (Figure 3B). Similar observations were made using the homozygous p.M771V ECFCs derived from the unrelated Person 7 (Supplementary Figure 1). In line with the impaired proteolytic processing was the lack of VWF secretion by the homozygous p.M771V ECFCs (Figure 3C), resulting in the severe bleeding phenotype. Interestingly, the amount of VWF secreted within 24 hours by heterozygous CB-ECFCs was comparable to the amount of VWF secreted by CB-ECFCs from healthy donors. Analysis of the multimeric composition of secreted VWF by agarose gel electrophoresis revealed a complete loss of HMW VWF multimers in homozygous p.M771V ECFCs (Figure 3C, D), with oligomers not extending beyond 10 subunits. Again, an intermediate phenotype was observed in the heterozygous p.M771V ECFCs, which had detectable but drastically decreased HMW VWF multimers. Taken together, these data indicate that the p.M771V variant is associated with defective proteolytic processing and multimerization due to ER retention of VWF, which negatively influences the secretion capacity of those cells.

3.3 | VWF p.M771V is retained in ER and unable to form pseudo-WPBs in HEK293 cells

To further corroborate our findings, we introduced WT VWF and p.M771V VWF in HEK293 cells. HEK293 cells are known to form pseudo Weibel-Palade bodies upon ectopic VWF expression and are a commonly used cell line to study the effect of VWF mutants on biosynthesis and trafficking [32]. Transfection of WT and mutant VWF in HEK293 cells generally resulted in a subset of cells expressing these constructs (Figure 4). As expected, HEK293 cells expressing WT VWF contained elongated pseudo-WPBs (Figure 4, top panel). However, p.M771V VWF expression in HEK293 cells was found distributed in a reticular pattern that colocalized with the ER marker PDI (Figure 4, bottom panel), resembling the ER retention phenotype that was observed in the patient ECFCs.

3.4 | CRISPR-Cas9 base editing in healthy CB-ECFCs

To further show that the p.M771V variant leads to impaired VWF processing, healthy CB-ECFCs were subjected to lentiviral-based CRISPR-Cas9 ABE using SpG-ABE8-M771V to introduce the c.A2311G nucleotide change (Figure 5A) into *VWF*. This resulted in endogenous expression of VWF carrying the pathogenic p.M771V variant. As a control, we used the lentiviral SpG-ABE8 vector without a gRNA, to exclude any involvement of the lentivirus or the ABE8 base editor on VWF expression. Based upon Sanger sequencing followed by EditR analysis [24], an average of 70.5% editing efficiency was observed in bulk populations of transduced ECFCs after antibiotic selection with puromycin (Figure 5B, C;
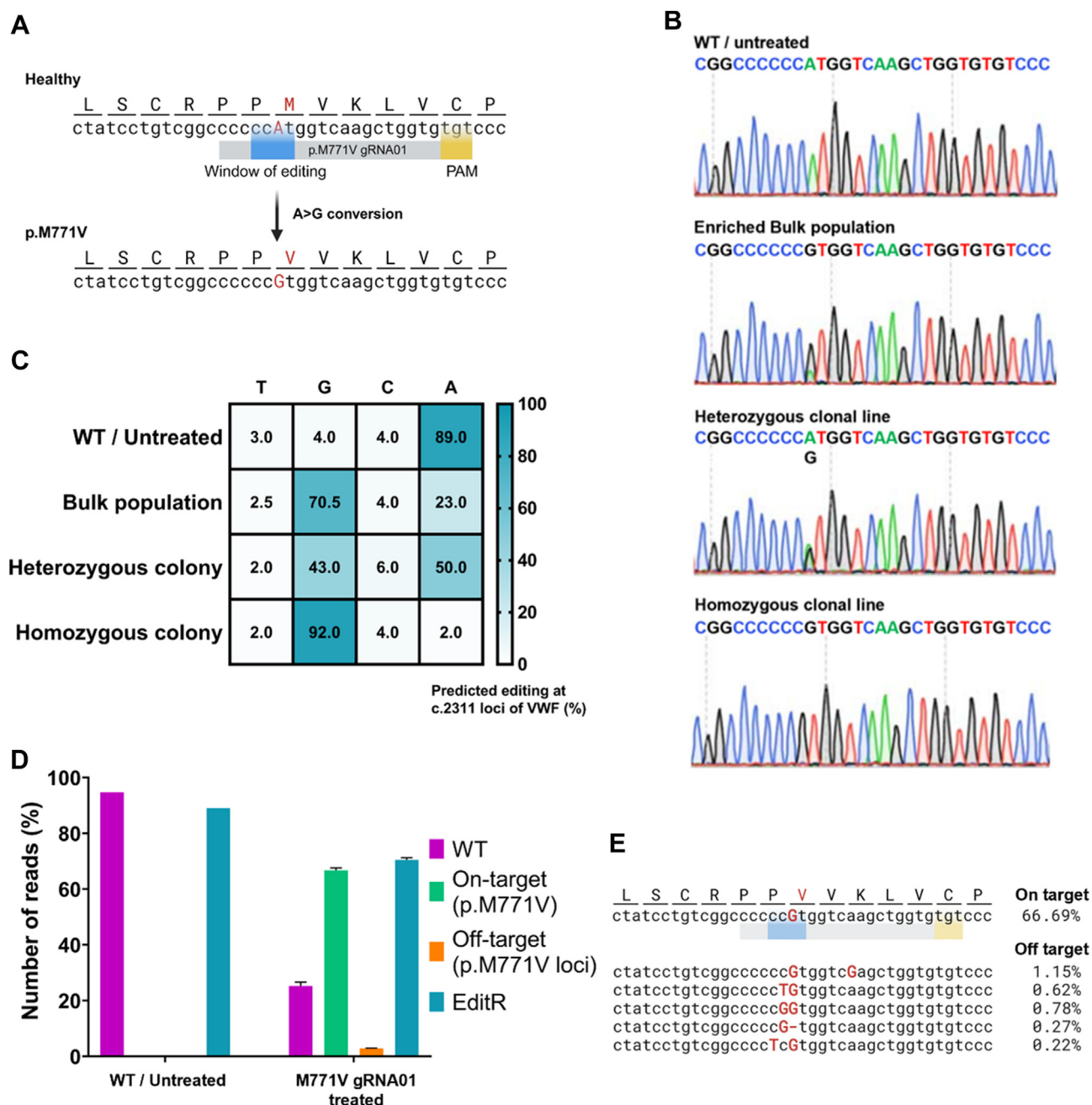
FIGURE 5 Introduction of patient variant p.M771V in healthy donor CB-ECFCs through CRISPR-Cas9 mediated base editing. (A) Overview of the gRNA designed to introduce p.M771V variant through the c.A2311G nucleotide substitution. (B) Sanger sequencing traces of an enriched bulk population and derived clonal lines at the p.M771V locus. (C) EditR quantification of Sanger sequencing traces from p.M771V bulk and clonal populations. (D) NGS quantification of edited alleles in an enriched bulk population. (E) Average off-targeting editing detected at the c.2311 loci through NGS based CRISPResso2 analysis of bulk populations. CB, cord blood; ECFC, endothelial colony-forming cell; gRNA, guide RNA; NGS, next generation sequencing; WT, wild type.

Supplementary Figures 2 and 3). For further validation, Illumina-based NGS was performed on enriched bulk populations in which an average of 66.69% on-target editing was detected (Figure 5D; Supplementary Figures 2 and 4). In addition, minimal off-targeting and bystander editing was seen at the p.M771V locus (Figure 5E). Through single cell sorting of the bulk populations, we also established clonal lines with homozygous and heterozygous p.M771V genotypes. This was confirmed by Sanger sequencing, and no bystander activity was present (Figure 5B, C).

Immunostaining was performed to assess how the frequency of p.M771V allele introduction impacts the VWF profile (Figure 6). Bulk populations displayed clear ER retention as most VWF colocalizes
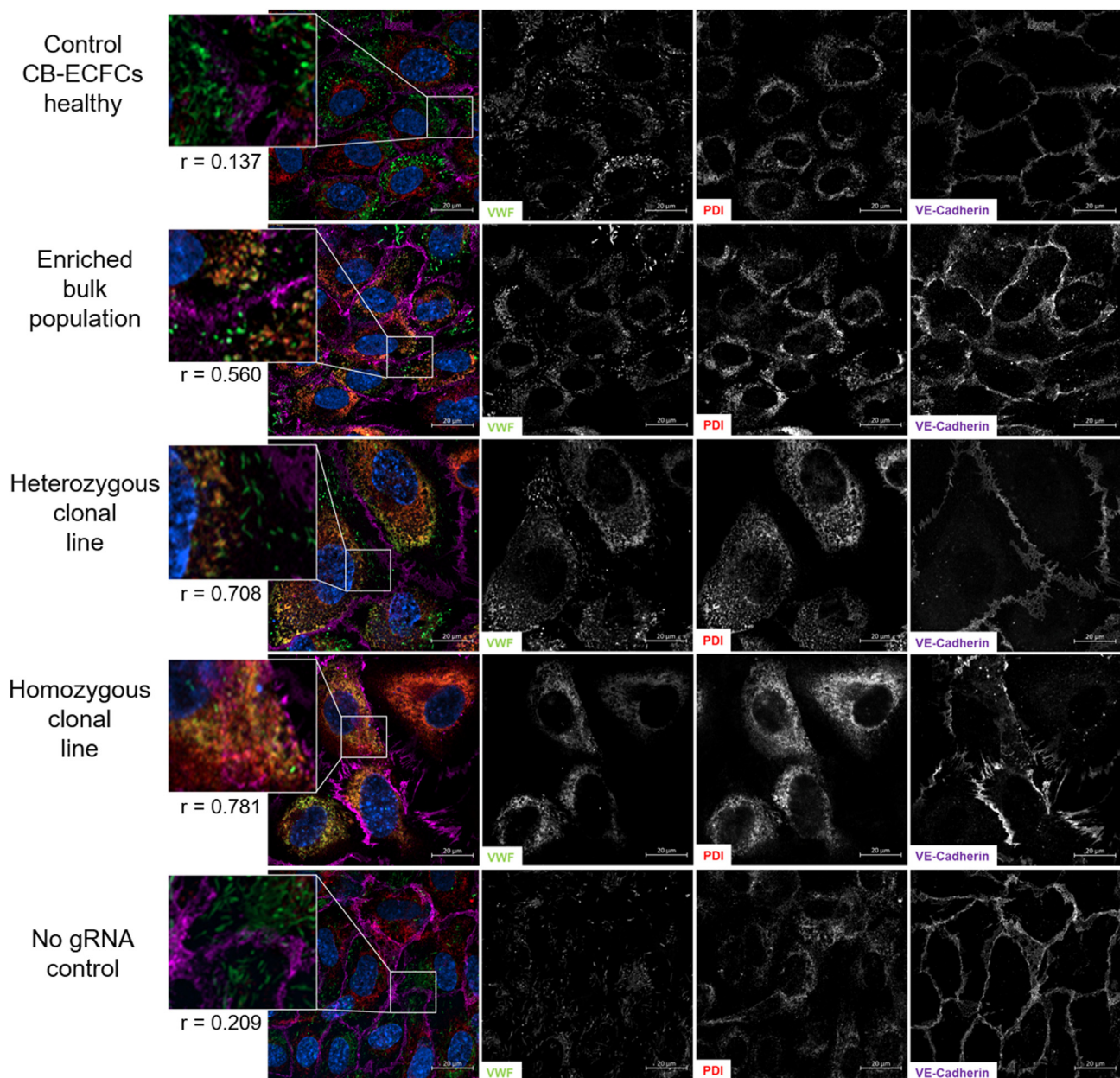
FIGURE 6 VWF profile of base-edited CB-ECFCs harboring the p.M771V variant. Immunostaining of CB-ECFC-enriched bulk and clonal populations predominantly show colocalization of VWF and PDI (ER marker) with absent WPBs. Clonal lines harboring a heterozygous genotype present with an intermediate phenotype. Magenta: VE-cadherin; Red: PDI; Green: VWF; scale bar 20 μm. Pearson's colocalization coefficient is represented by *r* value. CB, cord blood; ECFC, endothelial colony-forming cell; ER, endoplasmic reticulum; gRNA, guide RNA; PDI, protein disulfide isomerase; VE, vascular endothelial; WPB, Weibel-Palade body.

with PDI and scarce WPB formation can be seen. A control population was generated from ECFCs that were transduced with the vector lacking a gRNA and subsequently did not display any observable effects on VWF processing or formation of WPBs (Figure 6).

4 | DISCUSSION

When comparing heterozygous and homozygous p.M771V patient-derived ECFCs *in vitro* to ECFCs derived from healthy controls, we observed severe ER retention of VWF, resulting in impaired proVWF processing and a subsequent reduction of HMW multimers and secreted VWF. The WPBs observed in the heterozygous genotype were significantly shorter and rounder, suggesting a lower catalytic activity of stored VWF [30,33]. Studies have shown that inadequate Golgi VWF processing (eg, due to fragmentation of the Golgi) results in short WPBs harboring less and shorter VWF, subsequently leading to a lower catalytic activity [28,34]. The insufficient transport of VWF from the ER to the Golgi in the case of the p.M771V variant could have caused a phenotype similar to that in our study. These molecular

findings reflect the severe bleeding phenotype in homozygous p.M771V patients and explain the alleviated bleeding phenotype in heterozygous individuals.

Despite the severe bleeding in homozygous p.M771V individuals, it remains difficult to classify the type of VWD for those patients. Currently, diagnosis of VWD is mostly based on bleeding severity, coagulation laboratory findings, and the family history of bleeding problems, thereby rarely incorporating genetic testing. Ahmed et al. reported homozygous p.M771V patients in an Indian cohort that were diagnosed with VWD type 3, whereas those with heterozygous p.M771V were diagnosed with VWD type 1 [35–37]. However, the basis of this diagnosis is unclear, and the VWF:Ag levels of our participants were too high to justify a VWD type 3 diagnosis [38]. According to the American Society of Hematology, ISTH, National Hemophilia Foundation, and World Federation of Hemophilia 2021 guidelines, a VWF:FVIIIB test needs to be performed to diagnose VWD type 2N. However, the classification of the p.M771V variant as a pathogenic mutation would justify a type 2N VWD diagnosis based on its location in the FVIII-binding D'D3 domain [39]. Kakela et al. [40] reported a patient carrying the p.M771V variant that was diagnosed with VWD type 2N/1, and a previous study investigating VWF variants of patients enrolled in the 3 WINTERS-IPS study also mentioned the p.M771V variant in connection with type 2N/1 VWD [41]. However, we were unable to perform this analysis in our patients due to an insufficient amount of secreted VWF in plasma. In general, variants present at the p.M771 locus appear problematic as multiple studies have also diagnosed patients harboring heterozygous p.M771I variants as VWD type 1 [36,37]. Overall, the p.M771V variant seems difficult to classify based on the phenotype and plasma levels, which stresses the importance of unraveling the pathogenic mechanisms of VWD variants once more.

Individuals with the p.M771V variant present with elevated ratios of proVWF to mature VWF and a reduced amount of cleaved VWFpp. In this study, we discovered 2 possible mechanisms that hamper the cleavage of the VWFpp. First, the majority of produced VWF seems unable to proceed from the ER to the Golgi apparatus to undergo subsequent posttranslational modifications. The ER retention thereby also prevents cleavage of the VWFpp, which is then not detectable in lysates of homozygous p.M771V ECFCs. This hypothesis is further supported by the observed shortening of WPB length in the heterozygous p.M771V cells, which is remarkably similar to the phenotype observed in studies by Karampini et al. [29], where the rate of membrane fusion between ER and Golgi was decreased. Yadegari et al. [42] also demonstrated, using a HEK293 system that coexpressed healthy and mutant VWFpp variants, that impaired transit to the Golgi results in ER retention. Studies by Bowman et al. [27] of homozygous VWFpp variants that lead to ER retention of VWF similarly showed an intermediate phenotype in heterozygous patients that is comparable to our findings here.

The second potential impairment is the proximal location of the p.M771V variant to the furin cleavage site of the VWFpp in the D' domain, cleaving at residues R763-S764 [43]. Therefore, the p.M771V variant has the potential to negatively influence VWFpp cleavage and contribute to the lack of VWF processing in those endothelial cells. Other variants have been reported in the vicinity of the p.M771 locus that disrupt VWFpp cleavage. Variants at R763 and the R760 type 2N variants have been reported to disrupt cleavage by furin because they lie within its consensus sequence. For the R760C variant in BHK cells, it was shown that recombinant VWF could still be trafficked and stored in pseudo-WPBs, with normal intracellular levels. The secretion was reported to be affected, with heterozygous recombinant VWF WT/R760C having levels around 50% of WT. FVIII binding was deceased, with severity comparable to a heterozygous type 2N [43]. Interestingly, the R763A variant was shown to impair secretion by 70% and 40% in vivo and ex vivo respectively, whereas the R763G variant (also type 2N) abolished propeptide cleavage entirely in COS-7 cells [44]. Heterozygous patients displayed abnormal plasma multimers, suggesting retention of the propeptide [45]. Although these variants are classified as type 2N; these observations support the view that they also impact multimerization and secretion, just like p.M771V [36,37].

Berber et al. [46] found that the p.M771I variant results in a phenotype similar to what was observed in the patient ECFCs in this study. They proposed an alternative mechanism that involves the loss of hydrogen bonding between the sulfur atom on the Met and the NH backbone of L809 as a result of the Met to Ile conversion, which subsequently affects β sheet properties at this location. Similar to p.M771I, the conversion to Val results in a nonpolar amino acid lacking a sulfur atom. Adding to this hypothesis, online prediction tools like MUpro, which assess the protein-damaging nature of a variant, confirmed these observations for the p.M771V variant, which, with a negative score of −0.747, is predicted to decrease the protein structure stability [47]. Pathogenicity prediction tools like PolyPhen-2 and Align GVGD score the variant as possibly damaging and likely damaging, respectively. ClinVar suggests that the p.M771V variant is likely pathogenic but also mentions reports of "uncertain significance."

To shed some light on the pathogenicity of the p.M771V variant, we used 2 cell systems: ectopic expression of VWF containing p.M771V in HEK293 cells and mimicking the variant in CB-ECFCs by inducing the c.2311A>G substitution with a CRISPR/Cas9 adenine base editor. HEK293 cells are widely used to assess the molecular effects of VWF variants [42], as these cells do not endogenously express VWF but can process VWF and form so-called pseudo-WPBs upon VWF overexpression [48,49]. Expression of p.M771V VWF in HEK293 did not result in the biogenesis of pseudo-WPBs as observed for WT VWF (Figure 4). Instead, the unorganized structure of VWF and its colocalization with the ER marker PDI confirms the results obtained with the patient-derived ECFCs and strongly suggests a pathogenic property of the p.M771V variant independent of additional variants in VWF. However, several issues remain with the common approach of testing causality of VWF variants in the HEK293 system, including the complexity of mimicking heterozygous variants, which is particularly pertinent given that ~75% of the VWF variants in VWD are heterozygous. Moreover, physiologically appropriate

expression of VWF is difficult to achieve using a nonendothelial cell line such as HEK293, which is not endowed with the native physiological context of an endothelial cell.

The optimal environment to study the pathogenic mechanisms is the endothelial cell, which has been modeled by various investigators using the ECFC model system [27,32,42,50,51]. However, in some cases, VWD patient-derived ECFCs can be difficult to obtain, precluding such analysis. In this study, we therefore report for the first time on the use of gene-edited CB-ECFCs as a model system for VWD. We used CRISPR-Cas9 base editing to introduce a single A to G conversion to generate CB-ECFCs expressing the p.M771V variant. We utilized the SpG variant of Cas9 that has expanded genome targeting capabilities through a relaxed NGN PAM recognition sequence, which allows for specific targeting of the M771 locus [20]. Sanger sequencing with EditR analysis has been shown to accurately quantify base-editing frequencies at each position on a Sanger trace as a means of quantifying editing efficiency and was shown here to quantify editing at a similar level to NGS. Both in bulk populations as well as the homozygous p.M771V expressing clones, ER retention was observed, confirming the pathogenic mechanism observed in patient-derived ECFCs as well as in ectopic VWF expression studies in HEK293 cells. This was further supported by repeating the process in a second unrelated CB-ECFC line (Supplementary Figures 2-4).

Taken together, the ectopic VWF expression in HEK293 cells and the mimicked gene-edited CB-ECFCs confirm the pathogenic properties of the p.M771V variant. Therefore, we conclude that the second variant (p.R2663P) that is present in the individuals studied here does not contribute to the cellular phenotype. Interestingly, VWD type 3 patients carrying the p.M771V variant in an Indian cohort also possess a second variant, which is not considered pathogenic by itself but was suggested to contribute to the p.M771V phenotype [35]. In a study by Kakela et al. [40], a patient was identified that harbored the p.M771V and an additional p.R1566X variant [40]. In both studies, there was no mention of p.R2663P.

Here, we demonstrate that SpCas9-mediated base editing is a very efficient way to mimic a patient variant if primary ECFCs are not available or have challenging culturing requirements. This provides a novel approach that will improve characterization of patient variants in a true endothelial background. By manipulating endogenous expression of pathogenic VWF from a native cellular background, we can clearly examine the VWF profile and observe fully matured WPBs, something not clearly evident with HEK293 systems. Moreover, recreation of heterozygous and homozygous genotypes is possible, which cannot be achieved by overexpression with a constitutive promoter. In this case, we used this technology to confirm that the p.M771V variant is pathogenic and causes ER retention, leading to a severe bleeding phenotype in homozygous patients. The technology outlined in this study can be used to generate well-defined cellular models of VWD. These models can subsequently be used to monitor the effects of newly developed treatments that can either aim for corrective gene-editing or more broadly applicable gene transfer studies for curing VWD.

ORCID

Ruben Bierings https://orcid.org/0000-0002-1205-9689

X

Isabel Bär @IsabelBr12
Frank W.G. Leebeek @FLeebeek
Jan Voorberg @VoorbergJ
Ruben Bierings @rbierings; @WiN_Study_NL; @Clotterdam

REFERENCES

[1] Pokrovskaya ID, Rhee SW, Ball KK, Kamykowski JA, Zhao OS, Cruz DRD, Cohen J, Aronova MA, Leapman RD, Storrie B. Tethered platelet capture provides a mechanism for restricting circulating platelet activation to the wound site. *Res Pract Thromb Haemost.* 2023;7:100058.

[2] Pipe SW, Montgomery RR, Pratt KP, Lenting PJ, Lillicrap D. Life in the shadow of a dominant partner: the FVIII-VWF association and its clinical implications for hemophilia A. *Blood.* 2016;128:2007–16.

[3] Karampini E, Bierings R, Voorberg J. Orchestration of primary hemostasis by platelet and endothelial lysosome-related organelles. *Arterioscler Thromb Vasc Biol.* 2020;40:1441–53.

[4] Hordijk S, Carter T, Bierings R. A new look at an old body: molecular determinants of Weibel-Palade body composition and von Willebrand factor exocytosis. *J Thromb Haemost.* 2024;22:1290–303.

[5] Sadler JE. von Willebrand factor assembly and secretion. *J Thromb Haemost.* 2009;7(Suppl 1):24–7.

[6] Leebeek FWG, Eikenboom JCJ. von Willebrand's disease. *N Engl J Med.* 2016;375:2067–80.

[7] Du P, Bergamasco A, Moride Y, Truong Berthoz FT, Özen G, Tzivelekis S. von Willebrand disease epidemiology, burden of illness and management: a systematic review. *J Blood Med.* 2023;14:189–208.

[8] Atiq F, Boender J, Van Heerde WL, Tellez Garcia JM, Schoormans SC, Krouwel S, Cnossen MH, Laros-van Gorkom BAP, de Meris J, Fijnvandraat K, van der Bom JG, Meijer K, van Galen KPM, Eikenboom J, Leebeek FWG. Importance of genotyping in von Willebrand disease to elucidate pathogenic mechanisms and variability in phenotype. *Hemasphere.* 2022;6:e718.

[9] Przeradzka MA, Van Galen J, Ebberink EHTM, Hoogendijk AJ, Van Der Zwaan C, Mertens K, van den Biggelaar M, Meijer AB. D' domain region Arg782-Cys799 of von Willebrand factor contributes to factor VIII binding. *Haematologica.* 2020;105:1695–703.

[10] Laffan M, Sathar J, Johnsen JM. von Willebrand disease: diagnosis and treatment, treatment of women, and genomic approach to diagnosis. *Haemophilia*. 2021;27(Suppl 3):66–74.

[11] Martin-Ramirez J, Hofman M, Van Den Biggelaar M, Hebbel RP, Voorberg J. Establishment of outgrowth endothelial cells from peripheral blood. *Nat Protoc*. 2012;7:1709–15.

[12] Schillemans M, Kat M, Westeneng J, Gangaev A, Hofman M, Nota B, van Alphen FPJ, de Boer M, van den Biggelaar M, Margadant C, Voorberg J, Bierings R. Alternative trafficking of Weibel-Palade body proteins in CRISPR/Cas9-engineered von Willebrand factor-deficient blood outgrowth endothelial cells. *Res Pract Thromb Haemost*. 2019;3:718–32.

[13] Brinkman HJM, Mertens K, Holthuis J, Zwart-Huinink LA, Grijm K, Van Mourik JA. The activation of human blood coagulation factor X on the surface of endothelial cells: a comparison with various vascular cells, platelets and monocytes. *Br J Haematol*. 1994;87: 332–42.

[14] Bolte S, Cordelières FP. A guided tour into subcellular colocalization analysis in light microscopy. *J Microsc*. 2006;224:213–32.

[15] Schindelin J, Arganda-Carreras I, Frise E, Kaynig V, Longair M, Pietzsch T, Preibisch S, Rueden C, Saalfeld S, Schmid B, Tinevez JY, White DJ, Hartenstein V, Eliceiri K, Tomancak P, Cardona A. Fiji: an open-source platform for biological-image analysis. *Nat Methods*. 2012;9:676–82.

[16] Laan SNJ, Dirven RJ, Bürgisser PE, Eikenboom J, Bierings R. SYMPHONY consortium. Automated segmentation and quantitative analysis of organelle morphology, localization and content using CellProfiler. *PLoS ONE*. 2023;18:e0278009.

[17] Swinkels M, Hordijk S, Bürgisser PE, Slotman JA, Carter T, Leebeek FWG, Jansen AJG, Voorberg J, Bierings R. Quantitative super-resolution imaging of platelet degranulation reveals differential release of von Willebrand factor and von Willebrand factor propeptide from alpha-granules. *J Thromb Haemost*. 2023;21: 1967–80.

[18] Hewlett L, Zupančič G, Mashanov G, Knipe L, Ogden D, Hannah MJ, Carter T. Temperature-dependence of Weibel-Palade body exocytosis and cell surface dispersal of von Willebrand factor and its propolypeptide. *PLoS ONE*. 2011;6:e27314.

[19] Bierings R, van den Biggelaar M, Kragt A, Mertens K, Voorberg J, van Mourik JA. Efficiency of von Willebrand factor-mediated targeting of interleukin-8 into Weibel–Palade bodies. *J Thromb Haemost*. 2007;5:2512–9.

[20] Alves CRR, Ha LL, Yaworski R, Sutton ER, Lazzarotto CR, Christie KA, Reilly A, Beauvais A, Doll RM, de la Cruz D, Maguire CA, Swoboda KJ, Tsai SQ, Kothary R, Kleinstiver BP. Optimization of base editors for the functional correction of *SMN2* as a treatment for spinal muscular atrophy. *Nat Biomed Eng*. 2024;8:118–31.

[21] Sanjana NE, Shalem O, Zhang F. Improved vectors and genome-wide libraries for CRISPR screening. *Nat Methods*. 2014;11:783–4.

[22] Richter MF, Zhao KT, Eton E, Lapinaite A, Newby GA, Thuronyi BW, Wilson C, Koblan LW, Zeng J, Bauer DE, Doudna JA, Liu DR. Phage-assisted evolution of an adenine base editor with improved Cas domain compatibility and activity. *Nat Biotechnol*. 2020;38:883–91.

[23] Concordet JP, Haeussler M. CRISPOR: intuitive guide selection for CRISPR/Cas9 genome editing experiments and screens. *Nucleic Acids Res*. 2018;46:W242–5.

[24] Kluesner MG, Nedveck DA, Lahr WS, Garbe JR, Abrahante JE, Webber BR, Moriarity BS. EditR: a method to quantify base editing from Sanger sequencing. *CRISPR J*. 2018;1:239–50.

[25] Clement K, Rees H, Canver MC, Gehrke JM, Farouni R, Hsu JY, Cole MA, Liu DR, Joung JK, Bauer DE, Pinello L. CRISPResso2 provides accurate and rapid genome editing sequence analysis. *Nat Biotechnol*. 2019;37:224–6.

[26] Rawley O, Lillicrap D. Functional roles of the von Willebrand factor propeptide. *Hamostaseologie*. 2021;41:63–8.

[27] Bowman M, Casey L, Selvam SN, Lima PDA, Rawley O, Hinds M, Tuttle A, Grabell J, Iorio A, Walker I, Lillicrap D, James P. von Willebrand factor propeptide variants lead to impaired storage and ER retention in patient-derived endothelial colony-forming cells. *J Thromb Haemost*. 2022;20:1599–609.

[28] Ferraro F, Kriston-Vizi J, Metcalf DJ, Martin-Martin B, Freeman J, Burden JJ, Westmoreland D, Dyer CE, Knight AE, Ketteler R, Cutler DF. A two-tier Golgi-based control of organelle size underpins the functional plasticity of endothelial cells. *Dev Cell*. 2014;29:292–304.

[29] Karampini E, Bürgisser PE, Olins J, Mulder AA, Jost CR, Geerts D, Voorberg J, Bierings R. Sec22b determines Weibel-Palade body length by controlling anterograde ER-Golgi transport. *Haematologica*. 2021;106:1138–47.

[30] Kat M, Margadant C, Voorberg J, Bierings R. Dispatch and delivery at the ER-Golgi interface: how endothelial cells tune their hemostatic response. *FEBS J*. 2022;289:6863–70.

[31] Kat M, Karampini E, Hoogendijk AJ, Bürgisser PE, Mulder AA, van Alphen FPJ, Olins J, Geerts D, Van den Biggelaar M, Margadant C, Voorberg J, Bierings R. Syntaxin 5 determines Weibel-Palade body size and von Willebrand factor secretion by controlling Golgi architecture. *Haematologica*. 2022;107:1827–39.

[32] Laan SNJ, Lenderink BG, Eikenboom JCJ, Bierings R, SYMPHONY consortium. Endothelial colony-forming cells in the spotlight: insights into the pathophysiology of von Willebrand disease and rare bleeding disorders. *J Thromb Haemost*. 2024;22:3355–65.

[33] Naß J, Terglane J, Gerke V. Weibel Palade bodies: unique secretory organelles of endothelial cells that control blood vessel homeostasis. *Front Cell Dev Biol*. 2021;9:813995.

[34] Ferraro F, Mafalda Lopes da S, Grimes W, Lee HK, Ketteler R, Kriston-Vizi J, Cutler DF. Weibel-Palade body size modulates the adhesive activity of its von Willebrand Factor cargo in cultured endothelial cells. *Sci Rep*. 2016;6:32473.

[35] Ahmad F, Budde U, Jan R, Oyen F, Kannan M, Saxena R, Schneppenheim R. Phenotypic and molecular characterisation of type 3 von Willebrand disease in a cohort of Indian patients. *Thromb Haemost*. 2013;109:652–60.

[36] Goodeve AC, Eikenboom J, Castaman G, Rodeghiero F, Federici AB, Batlle J, Meyer D, Mazurier C, Goudemand J, Schneppenheim R, Budde U, Ingerslev J, Habart D, Vorlova Z, Holmberg L, Lethagen S, Pasi J, Hill F, Hashemi Soteh M, Baronciani L, et al. Phenotype and genotype of a cohort of families historically diagnosed with type 1 von Willebrand disease in the European study, Molecular and Clinical Markers for the Diagnosis and Management of Type 1 von Willebrand Disease (MCMDM-1VWD). *Blood*. 2007;109:112–21.

[37] White-Adams TC, Ng CJ, Jacobi PM, Haberichter SL, Di Paola JA. Mutations in the D'D3 region of *VWF* traditionally associated with type 1 VWD lead to quantitative and qualitative deficiencies of VWF. *Thromb Res*. 2016;145:112–8.

[38] James PD, Connell NT, Ameer B, Di Paola J, Eikenboom J, Giraud N, Haberichter S, Jacobs-Pratt V, Konkle B, McLintock C, McRae S, Montgomery RR, O'Donnell JS, Scappe N, Sidonio R, Flood VH, Husainat N, Kalot MA, Mustafa RA. ASH ISTH NHF WFH 2021 guidelines on the diagnosis of von Willebrand disease. *Blood Adv*. 2021;5:280–300.

[39] James P, Leebeek F, Casari C, Lillicrap D. Diagnosis and treatment of von Willebrand disease in 2024 and beyond. *Haemophilia*. 2024;30(Suppl 3):103–11.

[40] Kakela JK, Friedman KD, Haberichter SL, Buchholz NP, Christopherson PA, Kroner PA, Gill JC, Montgomery RR, Bellissimo DB. Genetic mutations in von Willebrand disease identified by DHPLC and DNA sequence analysis. *Mol Genet Metab*. 2006;87:262–71.

[41] Baronciani L, Peake I, Schneppenheim R, Goodeve A, Ahmadinejad M, Badiee Z, Baghaipour MR, Benitez O, Bodó I, Budde U, Cairo A, Castaman G, Eshghi P, Goudemand J, Hassenpflug W, Hoorfar H, Karimi M, Keikhaei B, Lassila R, Leebeek FWG, et al. Genotypes of European and Iranian patients with type 3 von Willebrand disease enrolled in 3WINTERS-IPS. *Blood Adv.* 2021;5:2987–3001.

[42] Yadegari H, Biswas A, Ahmed S, Naz A, Oldenburg J. von Willebrand factor propeptide missense variants affect anterograde transport to Golgi resulting in ER retention. *Hum Mutat.* 2021;42: 731–44.

[43] Casonato A, Sartorello F, Cattini MG, Pontara E, Soldera C, Bertomoro A, Girolami A. An Arg760Cys mutation in the consensus sequence of the von Willebrand factor propeptide cleavage site is responsible for a new von Willebrand disease variant. *Blood.* 2003;101:151–6.

[44] Swystun LL, Georgescu I, Mewburn J, Deforest M, Nesbitt K, Hebert K, Dwyer C, Brown C, Notley C, Lillicrap D. Abnormal von Willebrand factor secretion, factor VIII stabilization and thrombus dynamics in type 2N von Willebrand disease mice. *J Thromb Haemost.* 2017;15:1607–19.

[45] Hilbert L, Nurden P, Caron C, Nurden AT, Goudemand J, Meyer D, Fressinaud E, Mazurier C, INSERM Network on Molecular Abnormalities in von Willebrand Disease. Type 2N von Willebrand disease due to compound heterozygosity for R854Q and a novel R763G mutation at the cleavage site of von Willebrand factor propeptide. *Thromb Haemost.* 2006;96:290–4.

[46] Berber E, Ozbil M, Brown C, Baslar Z, Caglayan SH, Lillicrap D. Functional characterisation of the type 1 von Willebrand disease candidate *VWF* gene variants: p.M771I, p.L881R and p.P1413L. *Blood Transfus.* 2017;15:548–56.

[47] Cheng J, Randall A, Baldi P. Prediction of protein stability changes for single-site mutations using support vector machines. *Proteins.* 2006;62:1125–32.

[48] De Boer S, Eikenboom J. von Willebrand disease: from in vivo to in vitro disease models. *Hemasphere.* 2019;3:e297.

[49] Michaux G, Hewlett LJ, Messenger SL, Goodeve AC, Peake IR, Daly ME, Cutler DF. Analysis of intracellular storage and regulated secretion of 3 von Willebrand disease-causing variants of von Willebrand factor. *Blood.* 2003;102:2452–8.

[50] Starke RD, Paschalaki KE, Dyer CEF, Harrison-Lavoie KJ, Cutler JA, McKinnon TAJ, Millar CM, Cutler DF, Laffan MA, Randi AM. Cellular and molecular basis of von Willebrand disease: studies on blood outgrowth endothelial cells. *Blood.* 2013;121:2773–84.

[51] Wang JW, Bouwens EAM, Pintao MC, Voorberg J, Safdar H, Valentijn KM, de Boer HC, Mertens K, Reitsma PH, Eikenboom J. Analysis of the storage and secretion of von Willebrand factor in blood outgrowth endothelial cells derived from patients with von Willebrand disease. *Blood.* 2013;121:2762–72.

SUPPLEMENTARY MATERIAL

The online version contains supplementary material available at
https://doi.org/10.1016/j.jtha.2024.10.023